Journal of Optical Technology

Laser-induced improvement of the photoelectric characteristics of ZnO:Ag thin films

V. R. Gresko,[1,*] V. V. Smirnova,[1,3] M. M. Sergeev,[1,4] A. E. Pushkareva,[1,5] A. J. Dolgopolov,[1,6] L. A. Sokura,[1,7] and V. V. Bryukhanova[2,8]

[1]ITMO University, Institute of Laser Technologies, St. Petersburg, Russia
[2]Saint Petersburg State University, St. Petersburg, Russia
[3]smirnova1211.smirnova@yandex.ru
[4]mmsergeev@itmo.ru
[5]alexandra.pushkareva@gmail.com
[6]addolgopolov@itmo.ru
[7]sokuraliliy@mail.ru
[8]verabryu@gmail.com
*gresko.97@mail.ru

Received 30 September 2022; revised 12 December 2022; accepted 27 February 2023; Opticheskiĭ Zhurnal **90**, 57–67 (April 2023)

***Subject of study*. The paper considers the results of studies on the influence of the power density of continuous-wave laser emission on the optical and electrical characteristics of ZnO thin films with silver nanoparticles. *Aim of study*. The aim is improving the photoelectric characteristics of ZnO:Ag films by laser treatment to increase the efficiency of ultraviolet radiation photodetection. *Method*. The properties of ZnO:Ag films are modified using focused radiation with a wavelength of 405 nm in the scanning mode. The films are examined using optical and electron microscopy. Electrical resistance, dark current, and photocurrent arising from exposure to radiation with a wavelength of 343 nm are measured using a multimeter. *Main results*. It was deduced that the ratio of the photocurrent to dark current after exposure to radiation with a power density of 16 W/cm^2 increased from 4.8 to 7.4. The plasmon characteristics of the composite film changed, and the plasmon resonance peak shifted between 580 nm and 480 nm with increasing power density. The chemical composition of the film changed insignificantly after laser exposure. In this case, the film acquired a porous structure as the power density increased. *Practical significance*. The results obtained can be used to improve the efficiency of ultraviolet laser or solar radiation photodetectors based on ZnO:Ag films.**

https://doi.org/10.1364/JOT.90.000192

1. INTRODUCTION

Transparent conductive metal oxides (TCOs) have a unique combination of high transmission (approximately 80%) in the range from 400 nm to 1500 nm, associated with a large band gap of metal oxides (Eg > 3 eV), and high electrical conductivity (more than 10^3 1/(Ωcm)), close to the conductivity of some metals [1]. These properties allow for their application as transparent electrodes [2], in solar panels as window layers [3], photocatalysis [4], and information encryption devices [5].

Moreover, these materials are applied in the development of ultraviolet (UV) radiation photodetectors. One of the most common TCOs is ZnO [6,7], whose advantages include its relatively low cost and nontoxicity. Nevertheless, the lower conductivity of zinc oxide compared with other TCOs requires additional methods to increase it. Doping with metals, for example, Al [8], is often used, which increases the concentration of free charge carriers as well as the efficiency of the photodetector. An alternative to doping is the inclusion of metal nanoparticles in the film composition [9]. In the presence of nanoparticles, the Schottky effect and localized surface plasmon resonance (LSPR) can increase the concentration of free electrons, their lifetime, and carrier mobility [10], which also increases the efficiency of photodetection.

The modification of the film composition usually requires making changes to the material manufacturing process, such as additional doping operations or annealing in a furnace [11]. In most cases, this poses challenges during production with an already established technological process. Additionally, manufactured films may have defects that affect the quality of the final device. Laser irradiation serves as an additional tool for the rapid and highly efficient localized modification of film properties after their fabrication. It can affect both the TCO matrix [12] and the properties of the nanoparticles contained within it [13]. Depending on the parameters of laser irradiation, its effect can lead to either an improvement or a deterioration of the photovoltaic characteristics of the material.

The aim of this study was improving the photovoltaic characteristics of ZnO films with silver nanoparticles using laser irradiation to increase the efficiency of UV radiation photodetection.

2. METHODS AND MATERIALS

ZnO films with silver nanoparticles having an average diameter of approximately 40–50 nm (ZnO:Ag) on a fused quartz substrate with a thickness of 1 mm were used as the samples. The samples were prepared by the sol-gel method and annealed in a furnace at a temperature of 600°C. The film thickness was 120 nm.

The elements of the setup used in the experiment are shown in Fig. 1. An LSR405CP-2W semiconductor laser (*1*) with a wavelength of $\lambda = 405$ nm operating in continuous mode was used as the emission source. The emission was diaphragmed by a round hole (*2*), owing to which a round spot was formed. The emission was focused onto the sample surface (*5*) placed on a Thorlabs MTS50/M-Z8 movable three-coordinate table (*4*) using a 10× objective (*3*) with a focal length of $f = 5$ mm. Tracks that were 4 mm long were recorded on the surface at a scanning speed of $V = 4$ mm/s; the distance between adjacent tracks was 50 μm. The total modified area was 4×4 mm^2. The laser spot diameter was $d_0 =$ 20 μm. The power densities of the laser emission were $q = 16$ W/cm^2, 20 W/cm^2, 24 W/cm^2, 37 W/cm^2, 71 W/cm^2, 6300 W/cm^2, and 20,200 W/cm^2.

The emission power was measured using a UP19-H detector. The surface of the sample was examined using a Carl Zeiss Axio Imager optical microscope in the reflected and transmitted light modes. The surface morphology of the films was studied using a scanning electron microscope (SEM). The transmission T and reflection R of the films in the wavelength range from 400 to 800 nm were studied using an MSFU-K microscope-spectrophotometer. The chemical composition of the modified regions was studied through an energy dispersive detector (EDD) equipped with the SEM. The film resistivity was measured using a multimeter. To study the emerging photocurrent, the sample was irradiated with laser emission at a wavelength of 343 nm.

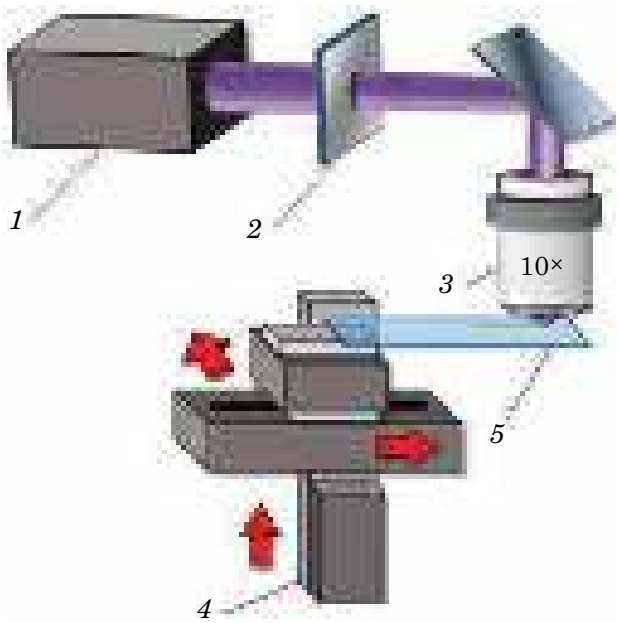

Fig. 1. Experimental scheme of laser film processing.

3. HEAT SOURCE SIMULATION

To elucidate the mechanism by which the structure and properties of films are altered through laser irradiation, an estimation was conducted on the size and shape of the heat source within the laser spot field, as well as the temperature gradient that facilitates the laser-induced modification of the film.

Numerical simulations were conducted using the Comsol software package and the finite element method to analyze the temperature fields generated during laser processing of the sample. The heat conduction equation, which considers a moving volumetric heat source along the x-axis, takes the following form:

$$\frac{\partial^2 T}{\partial \varepsilon^2} + \frac{\partial^2 T}{\partial \eta^2} + \frac{\partial^2 T}{\partial \xi^2} - \frac{V}{a}\frac{\partial T}{\partial \varepsilon} + \frac{W(\varepsilon, \eta, \xi)}{k} = \frac{1}{a}\frac{\partial T}{\partial t}, \quad (1)$$

where $\varepsilon = x - Vt$, $\eta = y$, and $\xi = z$ are the coordinates in the moving coordinate system, the center of which coincides with the center of the laser emission spot; $W(\varepsilon, \eta, \xi)$ is the volumetric power density of the internal heat source caused by the absorption of laser emission by the material; k is the thermal conductivity of the material; a is the thermal diffusivity of the material; and V is the velocity of the laser source equal to 4 mm/s. Equation (1) was solved for a two-layer medium, including a ZnO:Ag film (thickness of 120 nm, $k = 5.45$ W/mK, $a = 1.9 \times 10^{-6}$ m^2/s) and a substrate made of fused quartz (thickness of 1 mm, $k = 0.96$ W/mK, $a = 5.9 \times 10^{-7}$ m^2/s). The volumetric power density of the internal heat source caused by the absorption of the laser emission by the material was calculated in the cylindrical region under the impact spot as $W(z) = q\mu_a \exp(-\mu_a z)$, where μ_a is the absorption coefficient of the material obtained from the experimental values of $A_{\max}$. Heat dissipation from the heated region was achieved through conduction into the film and substrate. The model did not consider the dependences of the nanoparticle concentration and size, optical and thermophysical characteristics on the temperature, as well as the energy associated with phase transitions and heat sink to the surrounding environment. The results obtained are shown in Figs. 2 and 3.

At q up to 71 W/cm^2, the maximum temperatures reached approximate values of 800°C. This allows us to draw a conclusion about the thermal mechanism of laser action. At q greater than 6300 W/cm^2, the maximum temperatures were several orders of magnitude higher than the evaporation temperature of a similar material (1400°C) [14], which obviously did not correspond to the observed results. This discrepancy can be associated with a change in the thermophysical and optical constants during phase transitions and changes in the parameters of the nanoparticles during processing. The maximum temperature in the center of the spot was established after 0.3 s and then did not change [Fig. 2(b)]. It can also be observed that the heating intensity decreased rapidly with the distance from the center of the spot [Figs. 2(a) and 3].

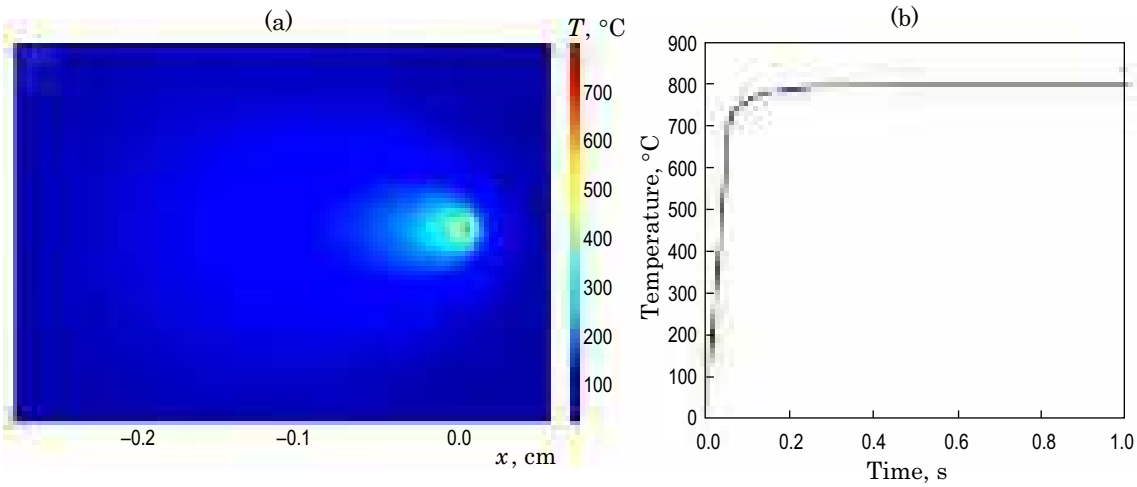

Fig. 2. Results of temperature modeling. (a) Temperature distribution over the sample's surface after 0.5 s from the start of processing at $q = 71$ W/cm^2, (b) time dependence of the temperature at the center of the laser spot on the sample surface.

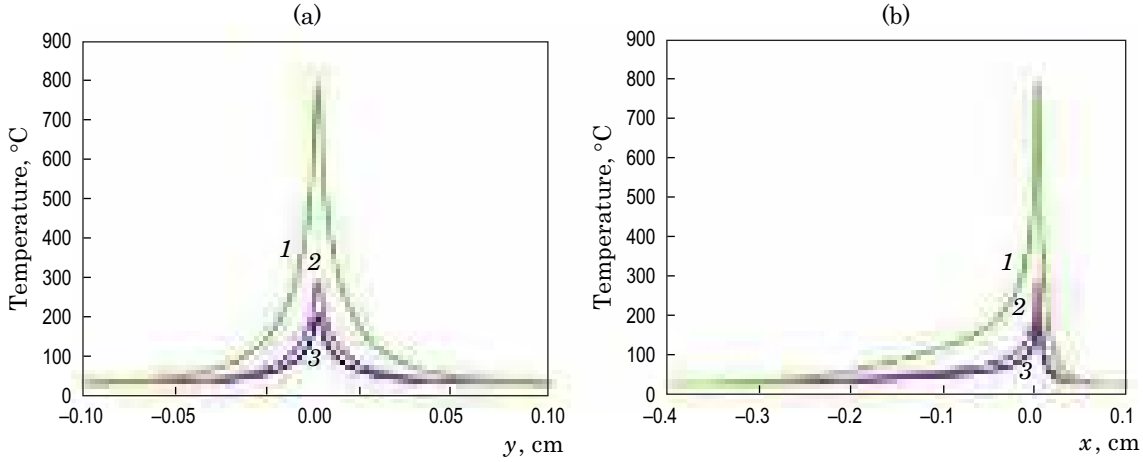

Fig. 3. Calculated temperature distribution over the surface of the sample as a result of exposure to laser radiation with a power density of 16 (curve *1*), 24 (curve *2*), and 71 W/cm^2 (curve*3*) 0.5 s after the start of processing. (a) Along the y-axis across the motion of the laser spot, (b) along the x-axis along the movement of the laser spot.

4. RESULTS AND DISCUSSION

One of the main factors influencing the result of laser exposure is the absorptivity of the material. Three main high-intensity regions can be distinguished in the absorption spectra of semiconductor films with metal nanoparticles. The first region is the intrinsic absorption region of the semiconductor, which corresponds to the interband optical transitions in the material. Normally UV emission falls into this region. The presence of the second region can be attributed to the occurrence of the plasmon resonance phenomenon in metal nanoparticles. This region is usually located in the visible light range. The third region of high absorption is near the plasma frequency of the material, which lies in the infrared wavelength range.

In the case of ZnO films with silver nanoparticles of a selected diameter, the wavelength of 405 nm does not fall within these three high absorption regions. It lies between the peak of the plasmon resonance and the edge of the intrinsic absorption region. Intense laser emission absorption on a ZnO matrix or on Ag particles can cause changes in the absorption capacity of the material. This can occur as a result of nanoparticle growth or destruction, as well as through the recrystallization of zinc oxide. This change in the absorptivity leads to nonlinear heating of the material. The use of a wavelength of 405 nm reduces the likelihood of such processes, allowing more controlled laser processing.

The surface of the film was examined using optical microscopy (Fig. 4). It was deduced that, at $q = 16$ W/cm^2, the reflection coefficient increased in the affected area. In turn, as q increased to 20,200 W/cm^2, the reflectance of the modified film decreased while the transmission increased. Because the modification of the film structure occurs owing to the thermal effect of emission, the results of processing can be compared with the results of thermal annealing of similar materials in a furnace. In [15], annealing at temperatures up to 700°C caused a decrease in the film thickness by 10 nm. Similar phenomena are possible under laser exposure. This makes it possible to assume that the change in the optical characteristics was associated with the change in the film thickness.

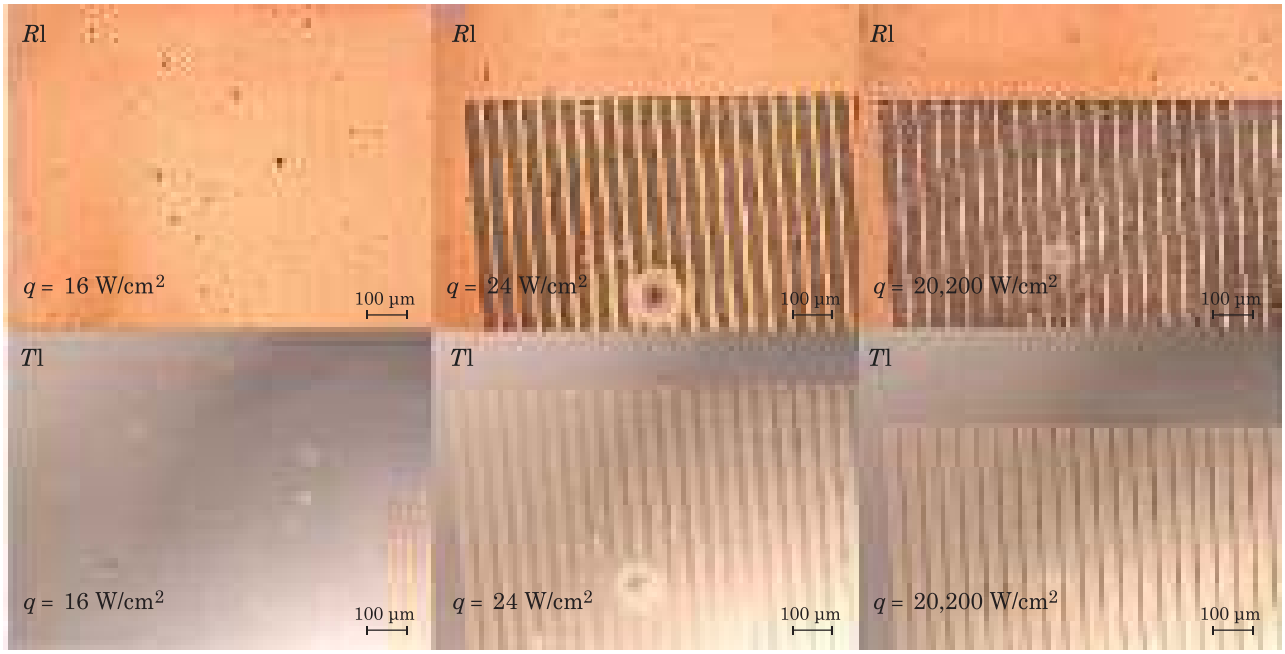

Fig. 4. Micrographs of ZnO:Ag film sections processed at different emission power densities in reflected (*R*l) and transmitted light (*T*l).

The morphological characteristics of the sample were studied using the SEM (Fig. 5). Simultaneously, a thin (5 nm) layer of carbon was deposited on the surface of the film to conduct the appropriate studies. The histograms of the size distribution of the nanoparticles are shown on the image of the initial film and the area processed with the maximum power density. As a result of laser treatment, the sizes of the silver nanoparticles decreased with increasing q. If, in the initial film, their average diameter was 40 nm, at the maximum q it became 20 nm. The concentration of nanoparticles also increased, which can be explained by the fact that the initial large nanoparticles were crushed into smaller ones during laser heating. Moreover, at power densities above 20 W/cm^2, structures resembling bubbles and pores were formed within the tracks.

The largest number of bubbles was observed in the films after treatment at $q = 20$ W/cm^2 (Fig. 6). As the power density increased, the number of bubbles in the center of the track decreased, whereas the number of pores increased. The appearance of pores and bubbles was likely associated with the thermal decomposition of zinc acetates and hydrates remaining after the sol-gel synthesis, accompanied by the release of gases (such as O_2 and CO_2) and water. Because the total film thickness is small and the scanning speed is high, only part of the gas comes to the surface and forms pores, whereas the remaining part remains in

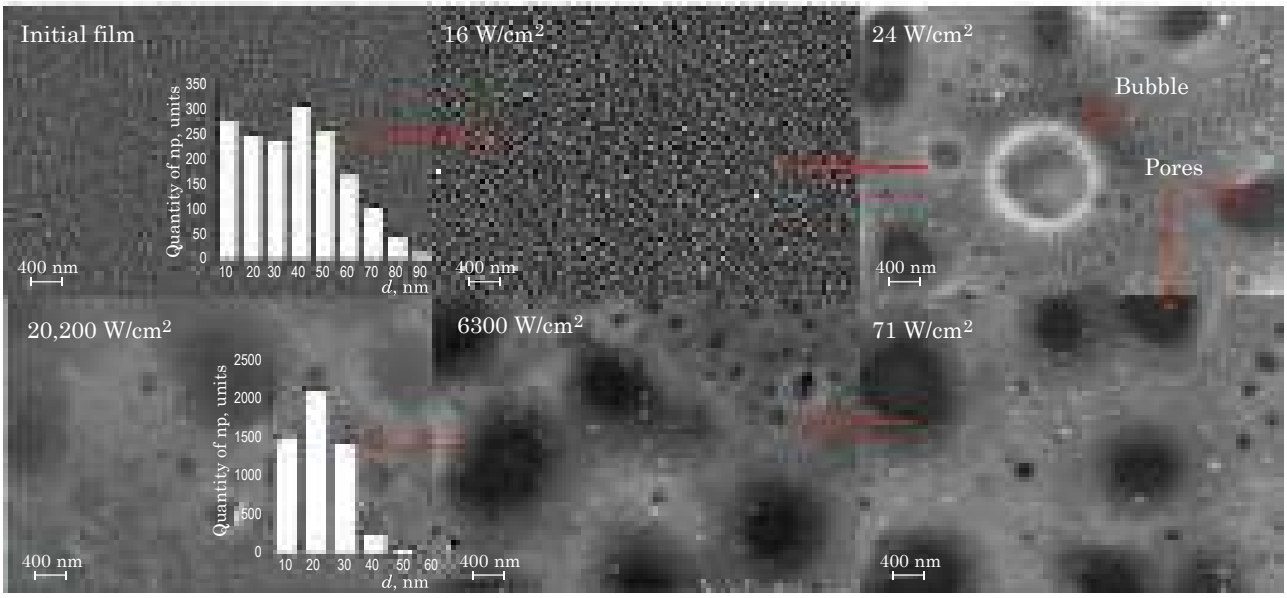

Fig. 5. SEM images of ZnO:Ag film after processing at various power densities.

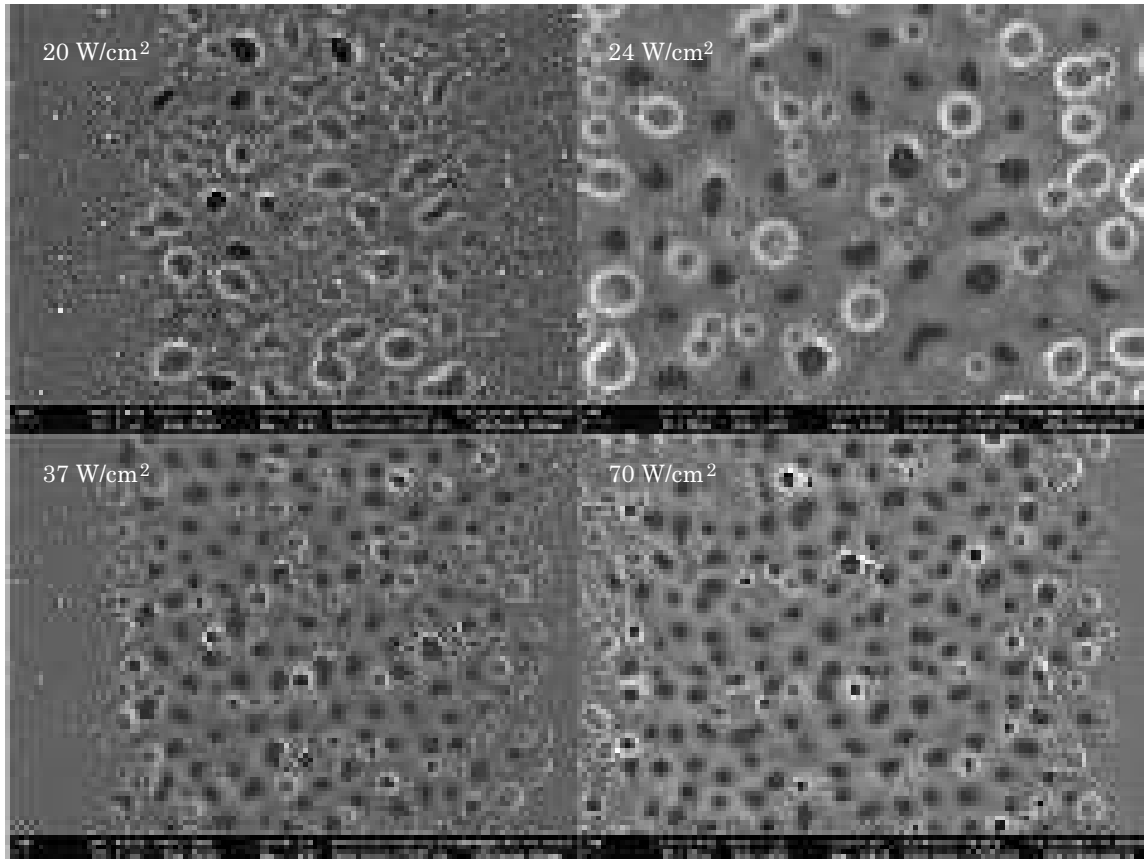

Fig. 6. Comparison of the pores and bubbles ratio on the SEM images of the ZnO:Ag film at different power densities.

the film thickness and forms bubbles. Increasing the processing power enhances thermal decomposition, making the formation of more pores and fewer bubbles possible.

Using an EDD, it was observed that the change in the content of all elements of the vibration was within 1%–3%. There was no silver in the pores, and the concentration of Zn also decreased, which is likely due to a local decrease in the film formation at the base of the pore. Silver was visible in the bubbles, but its concentration was lower than that in other areas.

Figure 7 shows the $A = 1 - T - R$ absorption spectra of the initial ZnO:Ag film and its modified regions. Figure 8 shows more detailed dependences of the absorption at the maximum of the plasmon peak A_{max} and wavelength at the maximum of the peak λ_{max} on the power density. The change in the spectral characteristics occurred both because of a change in the film thickness and the parameters of the nanoparticles. The blue shift of the absorption peak of the film (curves *3* and *4*), observed with an increase in the parameter q, was associated with the decay of large nanoparticles into smaller ones. As q increased to 20,200 W/cm^2 (curve *5*), the nanoparticles decayed into atoms and nanoclusters, as their contribution to the plasmon effects decreased, and the absorption at the peak maximum decreased as well. In this case, the absorption spectrum approached the spectrum of the ZnO film without nanoparticles.

The resistivity ρ_s of the samples was measured by the two-contact method (Fig. 9). The resistivity of the initial film was 0.23 Ωcm. The decrease in resistivity to 0.02 Ωcm at

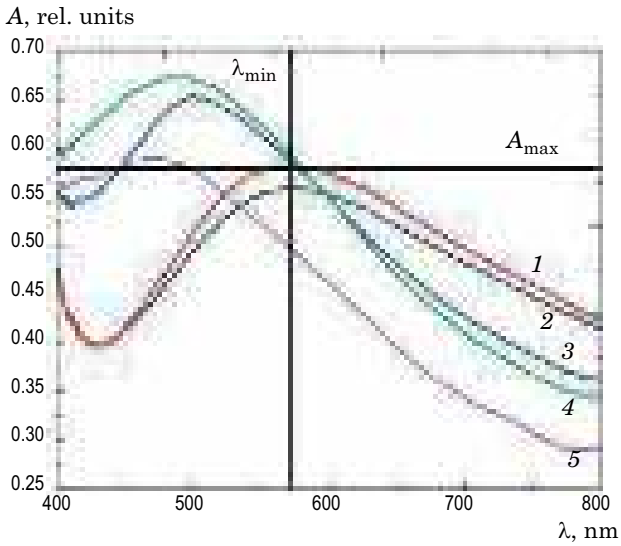

Fig. 7. Absorption spectra of the ZnO:Ag film at various power densities. Curve *1*—untreated film, curve *2*—16 W/cm^2, curve *3*—24 W/cm^2, curve *4*—71 W/cm^2, and curve *5*—20, 200 W/cm^2.

$q = 16$ W/cm^2 was associated with several reasons. First, under laser irradiation, electron emission from the silver nanoparticles into the ZnO matrix could occur [16]. This increased the charge carrier concentration and conductivity.

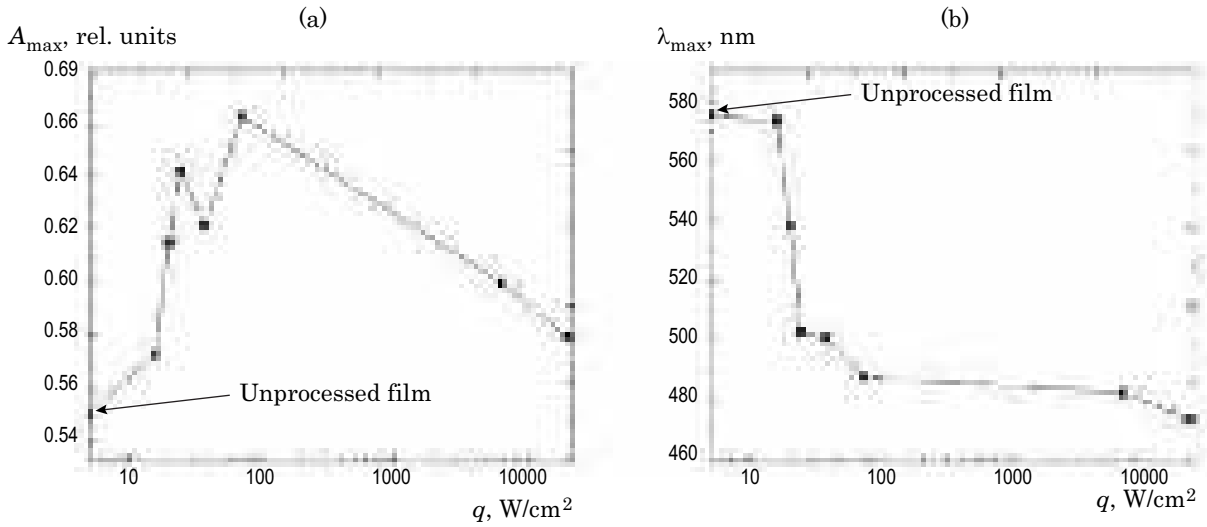

Fig. 8. Dependence of the plasmon resonance peak parameters on the power density q. (a) Dependence of A_{max} on q, (b) dependence of λ_{max} on q. The points are connected by lines for clarity.

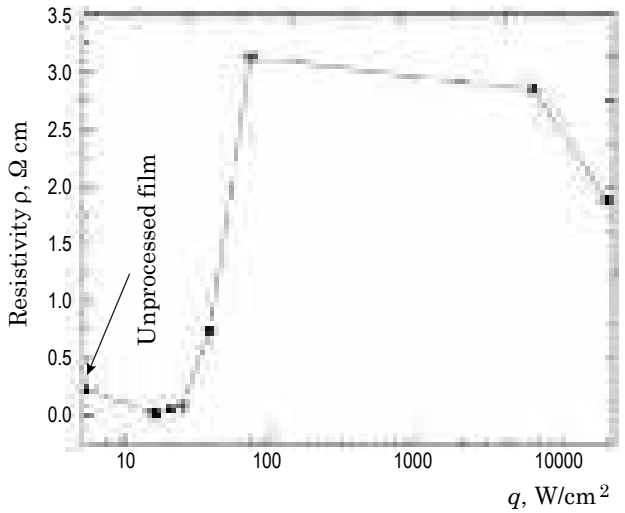

Fig. 9. Dependence of resistivity on emission power density for ZnO:Ag film annealed at 600°C. The points are connected by lines for clarity.

Secondly, under laser irradiation, part of the Zn–O bonds could be broken and oxygen vacancies V_o and interstitial zinc ions Zn_i could form [17]. These elements were free electron donors. Moreover, recrystallization of the ZnO structure could occur under the action of emission after reaching a sufficient temperature. Consequently, the crystallite size increased, and the number and thickness of the grain boundaries decreased, which increased the electron mobility [14]. A further increase in resistivity with an increase in the power density was associated with the pores formed in the film.

The region of the ZnO:Ag film with the lowest resistance was chosen to study the photocurrent from the action of UV radiation. The ratio of the photocurrent and dark current is one of the main parameters characterizing the efficiency of photodetectors. A pulsed laser with $\lambda = 343$ nm, pulse duration of $\tau = 224$ fs, and pulse repetition rate of $\nu = 1$ MHz was used to irradiate the sample. The average emission power was $P = 1.25$ W, and the pulse energy was $E = 1.25$ μJ. The impact occurred in a wide beam. The high-frequency mode of pulse generation was chosen so that the tested sections of the film acted as a detector of the average power of optical radiation. The dark current I_d of the sample was measured at the initial moment of time, in the absence of irradiation. The radiation was then turned on, and after 15 s, the value of the photocurrent I_{ph} was measured, followed by the laser turning off. Subsequently, after 30 s, the measurement was repeated.

As a result of the measurements, it was observed that the values of the dark current and photocurrent for the initial film were 20 ± 2 nA and 95 ± 5 nA, respectively. For the modified region, it was observed that $I_d = 38 \pm 1$ nA and $I_{ph} = 280 \pm 2$ nA. Thus, the I_{ph}/I_d ratio increased from 4.8 to 7.4 as a result of laser exposure.

5. CONCLUSION

In this study, continuous laser irradiation was employed to improve the photoelectric characteristics of thin ZnO films containing silver nanoparticles. It was demonstrated that the ratio of the photo- and dark currents increased after the irradiation of the sample with a UV laser. The modifications in the film properties were primarily attributed to the thermal effects induced by laser emission. Consequently, the surface morphology, spectral characteristics, and resistivity of the samples were altered, whereas the film composition experienced minimal changes. The findings from this study have the potential to enhance the efficiency of UV radiation photodetectors.

Funding. Russian Science Foundation (19-79-10208).

REFERENCES

1. H. Hosono and K. Ueda, "Transparent conductive oxides," in *Springer Handbook of Electronic and Photonic Materials*, S. Kasap and P. Capper, eds. (Berlin, 2017), pp. 1391–1404.

2. E. R. Rwenyagila, B. Agyei-Tuffour, K. M. G. Zebaze, O. Akin-Ojo, and W. O. Soboyejo, "Optical properties of ZnO/Al/ZnO multilayer films for large area transparent electrodes," J. Mater. Res. **29**(24), 2912–2920 (2014).
3. M. M. Islam, S. Ishizuka, A. Yamada, K. Matsubara, S. Niki, T. Sakurai, and K. Akimoto, "Thickness study of Al:ZnO film for application as a window layer in $Cu(In_{1-x}Ga_x)Se_2$ thin film solar cell," Appl. Surf. Sci. **257**(9), 4026–4030 (2011).
4. H. Karimi-Maleh, B. G. Kumar, S. Rajendran, J. Qin, S. Vadivel, D. Durgalakshmi, F. Gracia, M. Soto-Moscoso, Y. Orooji, and F. Karimi, "Tuning of metal oxides photocatalytic performance using Ag nanoparticles integration," J. Mol. Liq. **314**, 113588 (2011).
5. J. H. Castro-Chacón, C. Torres-Torres, A. V. Khomenko, M. A. García-Zárate, M. Trejo-Valdez, H. Martínez-Gutiérrez, and R. Torres-Martínez, "Encryption of nonlinear optical signals in ZnO:Al thin films by ultrashort laser pulses," J. Mod. Opt. **64**(6), 601–608 (2017).
6. K. Liu, M. Sakurai, and M. Aono, "ZnO-based ultraviolet photodetectors," Sensors **10**(9), 8604–8634 (2010).
7. Q. Li, J. Huang, J. Meng, and Z. Li, "Enhanced performance of a self-powered ZnO photodetector by coupling LSPR-inspired pyro-phototronic effect and piezo-phototronic effect," Adv. Opt. Mater. **10**(7), 2102468 (2022).
8. S. Singh and S. H. Park, "Fabrication and characterization of Al:ZnO based MSM ultraviolet photo-detectors," Superlattices Microstruct. **86**, 412–417 (2015).
9. N. P. Klochko, K. S. Klepikova, I. V. Khrypunova, V. R. Kopach, I. I. Tyukhov, S. I. Petrushenko, S. V. Dukarov, V. M. Sukhov, M. V. Kirichenko, and A. L. Khrypunova, "Solution-processed flexible broadband ZnO photodetector modified by Ag nanoparticles," Sol. Energy **232**, 1–11 (2022).
10. S.-K. Tzeng, M.-H. Hon, and I.-C. Leu, "Improving the performance of a zinc oxide nanowire ultraviolet photodetector by adding silver nanoparticles," J. Electrochem. Soc. **159**(4), H440 (2012).
11. D. Kim and J. Y. Leem, "Crystallization of ZnO thin films via thermal dissipation annealing method for high-performance UV photodetector with ultrahigh response speed," Sci. Rep. **11**(1), 382 (2021).
12. Q. Nian, M. Y. Zhang, B. D. Schwartz, and G. J. Cheng, "Ultraviolet laser crystallized ZnO:Al films on sapphire with high Hall mobility for simultaneous enhancement of conductivity and transparency," Appl. Phys. Lett. **104**(20), 201907 (2014).
13. N. Destouches, N. Crespo-Monteiro, G. Vitrant, Y. Lefkir, S. Reynaud, T. Epicier, Y. Liu, F. Vocanson, and F. Pigeon, "Self-organized growth of metallic nanoparticles in a thin film under homogeneous and continuous-wave light excitation," J. Mater. Chem. **2**(31), 6256–6263 (2014).
14. M. Y. Zhang and G. J. Cheng, "Highly conductive and transparent alumina-doped ZnO films processed by direct pulsed laser recrystallization at room temperature," Appl. Phys. Lett. **99**(5), 051904 (2011).
15. L. A. Sokura, E. V. Shirshneva-Vaschenko, D. A. Kirilenko, Z. G. Snezhnaia, P. S. Shirshnev, and A. E. Romanov, "Electron-microscopy study of ordered silver nanoparticles synthesized in a ZnO:Al polycrystalline film," J. Phys.: Conf. Ser. **1410**(1), 012170 (2019).
16. C. S. Hong, H. H. Park, and H. J. Chang, "Optical and electrical properties of ZnO thin film containing nano-sized Ag particles," J. Electroceram. **22**(4), 353–356 (2009).
17. Y. Zhao and Y. Jiang, "Effect of KrF excimer laser irradiation on the properties of ZnO thin films," J. Appl. Phys. **103**(11), 114903 (2008).

Vladislav R. Gresko—Research Engineer, ITMO University, 197101, St. Petersburg, Russia; Scopus ID: 57211848411, http://orcid.org/0000-0003-3308-6034, gresko.97@mail.ru

Lilia A. Sokura—Engineer, ITMO University, 197101, St. Petersburg, Russia; Scopus ID: 56662497100, http://orcid.org/0000-0001-9725-5912, sokuraliliy@mail.ru

Aleksandra E. Pushkareva—Ph.D., Lead Engineer, ITMO University, 197101, St. Petersburg, Russia; Scopus ID: 12791000500, http://orcid.org/0000-0003-0082-984X, alexandra.pushkareva@gmail.com

Maksim M. Sergeev—Ph.D., Docent, Senior Researcher, ITMO University, 197101, St. Petersburg, Russia; http://orcid.org/0000-0003-2854-9954, mmsergeev@itmo.ru

Arthur D. Dolgopolov—Engineer, ITMO University, 197101, St. Petersburg, Russia; http://orcid.org/0000-0002-9548-791X, addolgopolov@itmo.ru

Viktoriia V. Smirnova—Senior Assistant, ITMO University, 197101, St. Petersburg, Russia; http://orcid.org/0000-0002-0349-2296, smirnova1211.smirnova@yandex.ru

Vera V. Bryukhanova—Engineer, Saint Petersburg State University, 199034, St. Petersburg, Russia; http://orcid.org/0000-0002-9862-1387, verabryu@gmail.com